Supporting information

Mitochondria-targeted ruthenium(II) complexes for photodynamic therapy and GSH detection in living cells

*Wanqing Zhang, Weibin Chen, Fengfu Fu, Mei-Jin Li**

Materials and chemicals

The chemicals used were purchased from commercial suppliers and used directly without purification. 9,10-anthracenediyl-bis(methylene)dimalonic acid (ABDA)， 1,3-Diphenylisobenzofuran (DPBF) and N-methylmaleimide (NEM) were purchased from Adamas Chemical Co. Cysteine (Cys), homocysteine (Hcy) and selenium oxide (SeO_2) were purchased from Alfa Aesar Chemical Co. Glutathione (GSH) and Glutathione oxydized (GSSG) were purchased from Acros Organics. Ammonium hexafluorophosphate (NH_4PF_6) and arginine hydrochloride (Arg), methionine (Met), phenylalanine (Phe), tryptophan (Trp), threonine (Thr), valine (Val), leucine (Leu), histidine hydrochloride (His), isoleucine (Ile), lysine hydrochloride (Lys) were purchased from Sigma-Aldrich. Homocysteine (Hcy) was purchased from Tokyo Chemical Industry (TCL). CCK-8 was purchased from MedChemExpress LLC (China). MitoTracker Green FM was purchased from Next Sense Biotechnology (Shanghai) Co. Phosphate buffered saline (PBS) was purchased from Cellmax Chemical Co. 4,4-Dimethyl-2,2-bipyridine, $RuCl_3$ was purchased from Aladdin Reagent Co. 4-Methyl-2,2-bipyridine-4-carboxaldehyde and $Ru(bpy)_2Cl_2$ were synthesized according to previously reported methods.[1] All other chemical reagents were of analytical grade and used directly without treatment.

Instruments

^{1}H NMR and ^{13}C NMR spectra were measured by JEOL (500 MHz) with

* Corresponding author. *E-mail address: mjli@fzu.edu.cn*

Me_4Si as internal standard. High resolution mass spectra (ESI-MS) were measured on a Thermo Finnigan DECAV-30000LCQ Deca XP mass spectrometer. Photoluminescence (PL) spectra and UV-visible absorption spectra were obtained on an Edinburgh FS5 EVOLUTION 220 and UV-visible spectrophotometer tests, and lifetimes were measured with an Edinburgh FLS920 spectrofluorometer. Crystal X-ray diffraction data were collected by a Bruker SMART diffractometer.

Cytotoxicity

Calculation formula for cell viability:

$$\text{Cell viability (\%)} = [(As-Ab) / (Ac-Ab)] \times 100\%.$$

Where As: absorbance of experimental wells (with cells and complexes);

Ac: absorbance of control group (with cells);

Ab: absorbance of blank group (without cells and complexes).

Synthesis

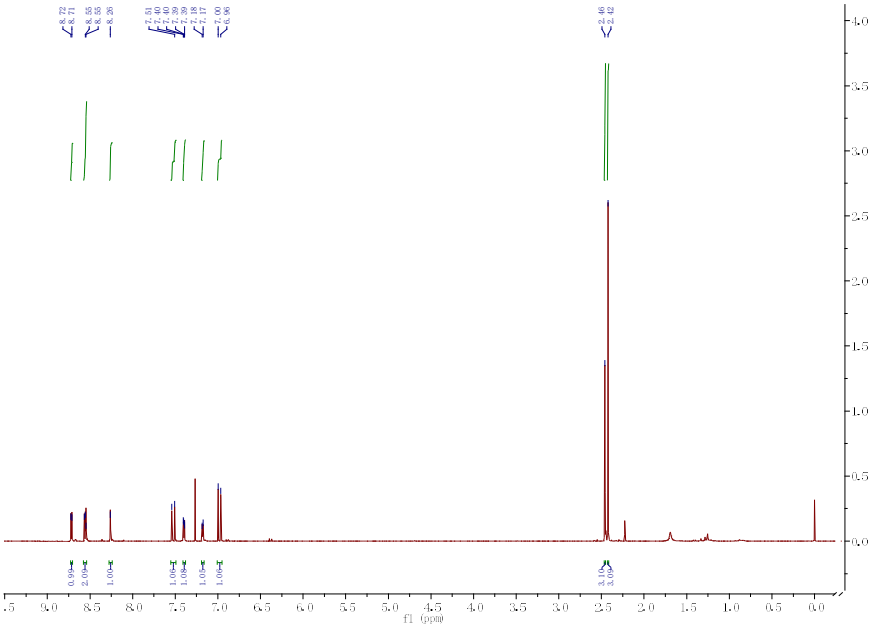

Fig. S1 ^{1}H NMR (500 MHz, $CDCl_3$) spectrum of ligand **1.**

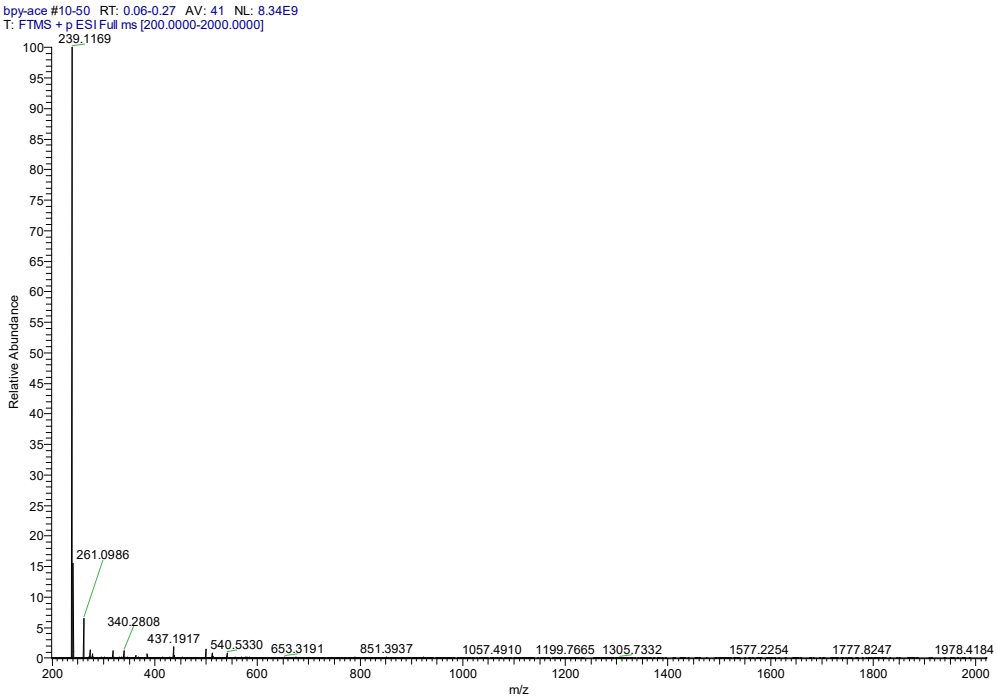

Fig. S2 ESI-MS of ligand **1** in dichloromethane solution at room temperature: m/z=239.1169$\{M+H\}^+$.

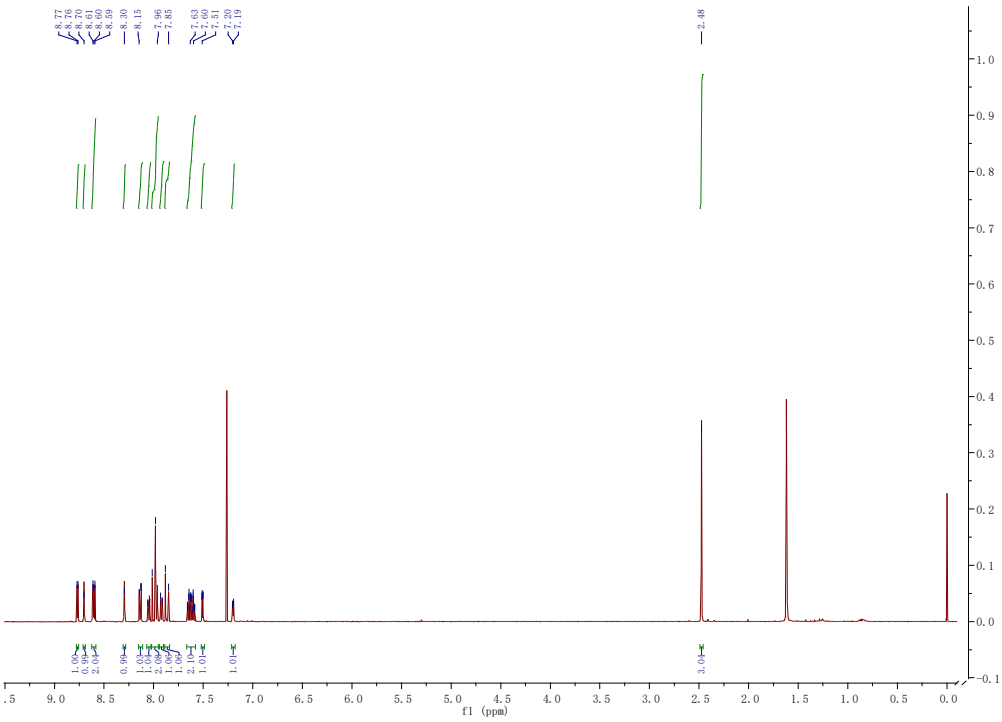

Fig. S3 ^{1}H NMR (500 MHz, $CDCl_3$) spectrum of ligand **2.**

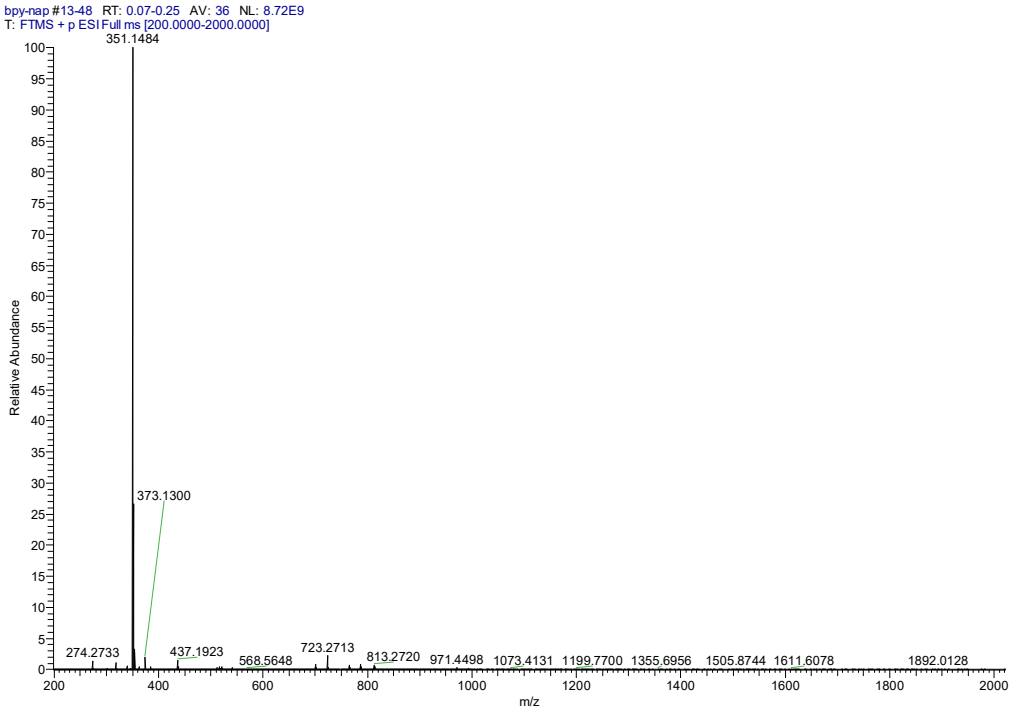

Fig. S4 ESI-MS of ligand **2** in dichloromethane solution at room temperature: m/z=351.1484$\{M+H\}^+$.

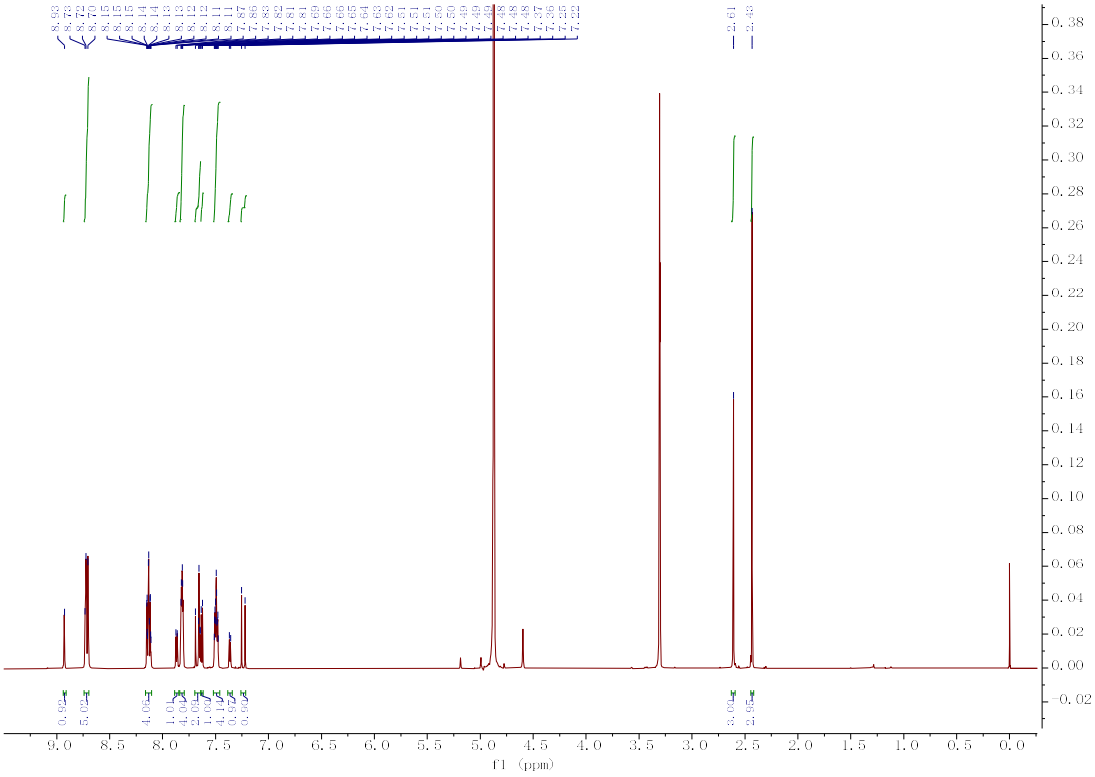

Fig. S5(a) ^{1}H NMR (500 MHz, methanol-d_4) spectrum of **Ru-1.**

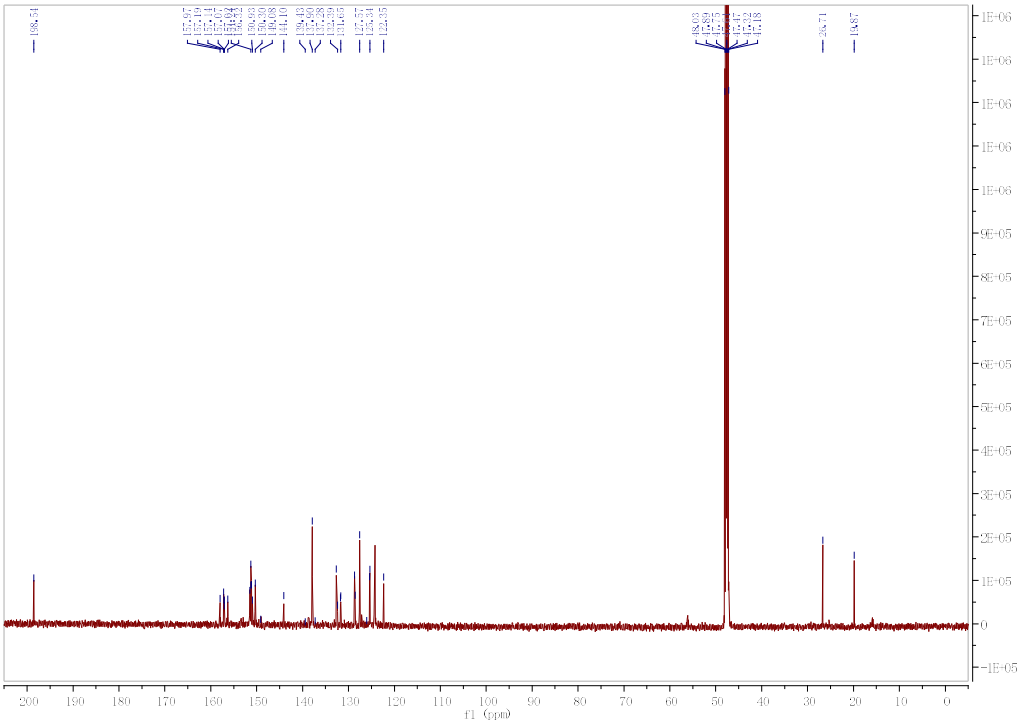

Fig. S5(b) ^{13}C NMR (151 MHz, methanol-d_4) spectrum of **Ru-1.**

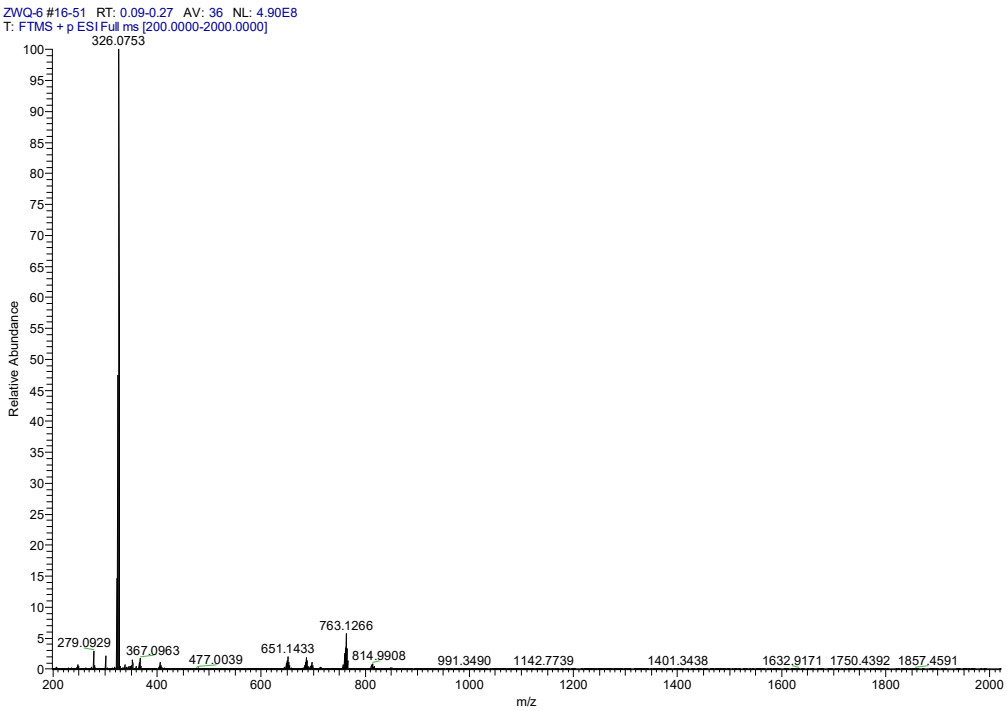

Fig. S6 ESI-MS of **Ru-1** in aqueous solution at room temperature: m/z=326.0753 $\{M\text{-}Cl_2\}^{2+}$.

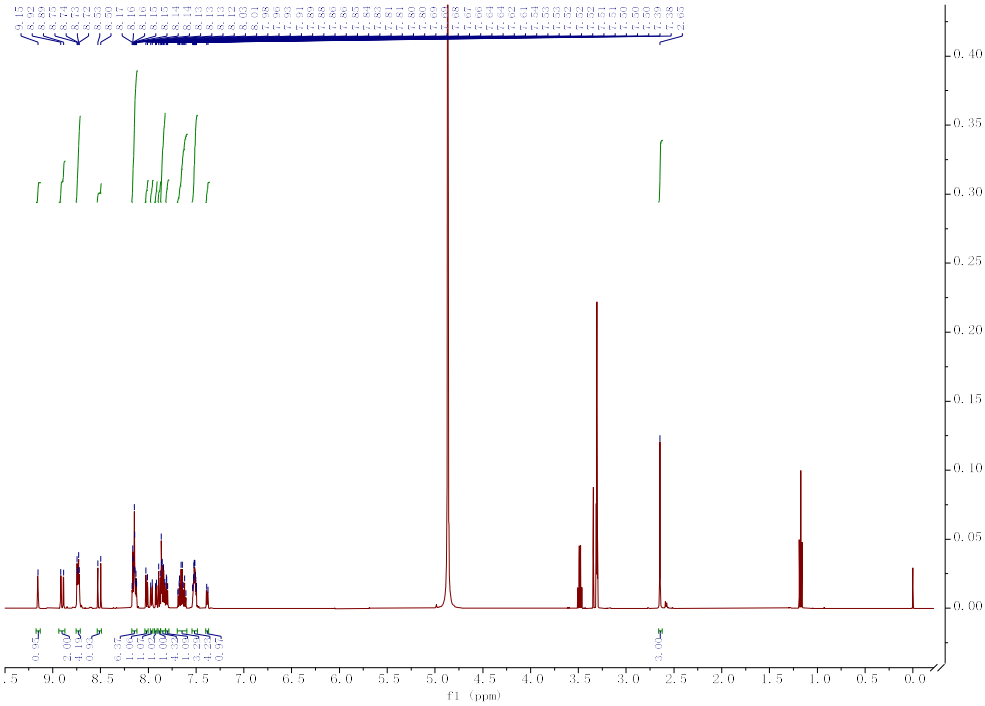

Fig. S7(a) ^{1}H NMR (500 MHz, Methanol-d_4) spectrum of **Ru-2.**

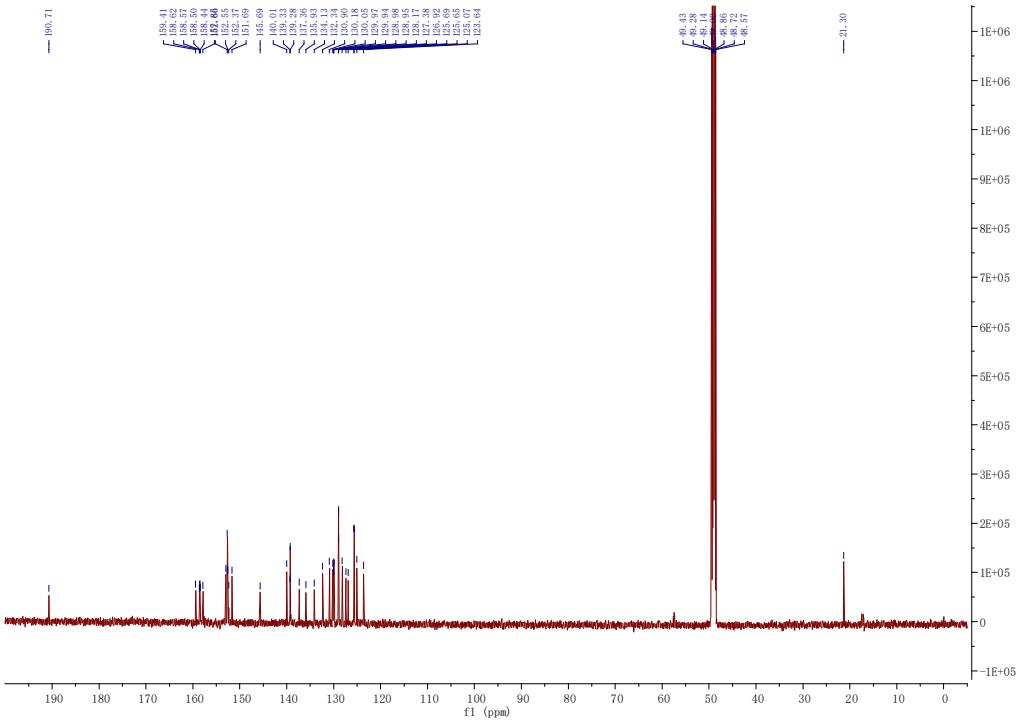

Fig.S7(b) ^{13}C NMR (151 MHz, Methanol-d_4) spectrum of **Ru-2.**

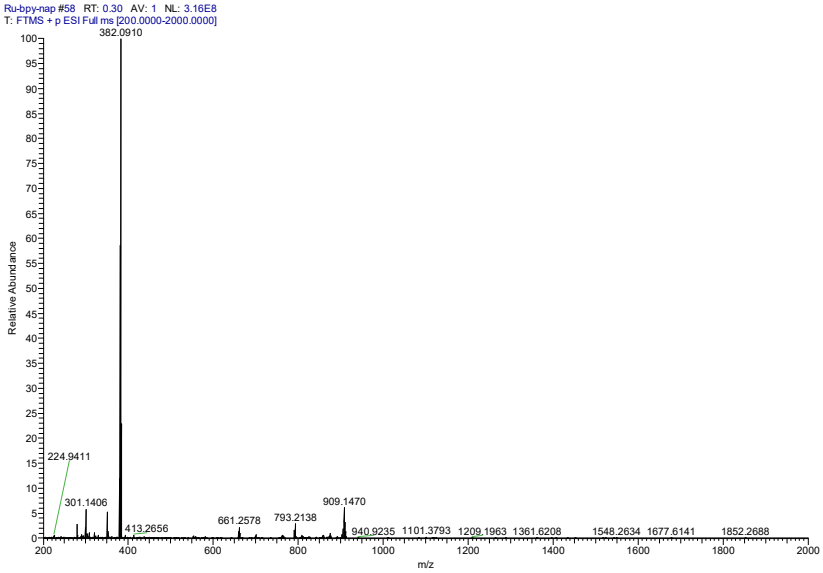

Fig. S8 ESI-MS of **Ru-2** in aqueous solution at room temperature: m/z=382.0910$\{M\text{-}Cl_2\}^{2+}$.

Table S1 Crystallographic data ang structural refinement data

Complex	**Ru-1**	**Ru-2**
Identification code	$[Ru(bpy)_2ligand1](PF_6)_2$	$[Ru(bpy)_2ligand2](PF_6)_2$
Empirical formula	$C_{37.1}H_{38.4}F_{12}N_6O_{3.1}P_2Ru$	$C_{44}H_{36.4}F_{12}N_6O_{2.2}P_2Ru$
Formula weight	1008.95	1075.40
Temperature/K	296.15	296.15
Crystal system	triclinic	triclinic
Space group	P-1	P-1
a/Å	10.8450(6)	9.9020(17)
b/Å	11.8133(7)	12.910(2)
c/Å	17.1597(9)	18.288(3)
α/°	86.824(2)	88.353(5)
β/°	82.482(2)	74.769(5)
γ/°	73.339(2)	87.246(5)
Volume/$Å^3$	2087.7(2)	2252.8(7)
Z	2	2
$\rho_{cal.}$g/cm^3	1.605	1.585
μ/mm^{-1}	0.551	0.515
F(000)	1020.0	1084.0
Crystal size/mm^3	0.16 × 0.14 × 0.1	0.18 × 0.15 × 0.1
Radiation	MoKα(λ = 0.71073)	MoKα(λ = 0.71073)
2Θ range for data collection/°	3.6 to 50.172	3.882 to 50.336

Index ranges	$-12 \leq h \leq 12$, $-14 \leq k \leq 14$, $-20 \leq l \leq 20$	$-11 \leq h \leq 11$, $-15 \leq k \leq 15$, $-21 \leq l \leq 21$
Reflections collected	53627	60521
Independent reflections	7388 [R_{int} = 0.0305, R_{sigma} = 0.0201]	8056 [R_{int} =0.0577, R_{sigma} = 0.0384]
Data/restraints/parameters	7388/465/575	8056/25/597
Goodness-of-fit on F^2	1.042	1.141
Final R indexes [I>=2σ (I)]	R_1 = 0.0532, wR_2 = 0.1277	R_1 = 0.0644, wR_2 = 0.1667
Final R indexes [all data]	R_1 = 0.0602, wR_2 = 0.1353	R_1 = 0.1112, wR_2 = 0.2204

Table S2 Selected bond lengths (Å) and angles (°) for **Ru-1 and Ru-2**

Ru-1		**Ru-2**	
Ru1-N4	2.060(3)	Ru1-N5	2.037(5)
Ru1-N2	2.059(3)	Ru1-N3	2.053(5)
Ru1-N5	2.055(3)	Ru1-N4	2.049(5)
Ru1-N1	2.061(3)	Ru1-N6	2.061(5)
Ru1-N3	2.064(3)	Ru1-N2	2.062(5)
Ru1-N6	2.052(3)	Ru1-N1	2.061(5)
C32-C33	1.328(7)	C32-C33	1.304(9)
O1-C34	1.217(7)	O1-C34	1.220(8)
N2-Ru1-N1	78.91(13)	N5-Ru1-N4	78.22(19)
N5-Ru1-N6	78.83(13)	N1-Ru1-N2	79.0(2)
N3-Ru1-N4	78.64(13)	N3-Ru1-N6	78.65(18)

Sensing of GSH by complexes

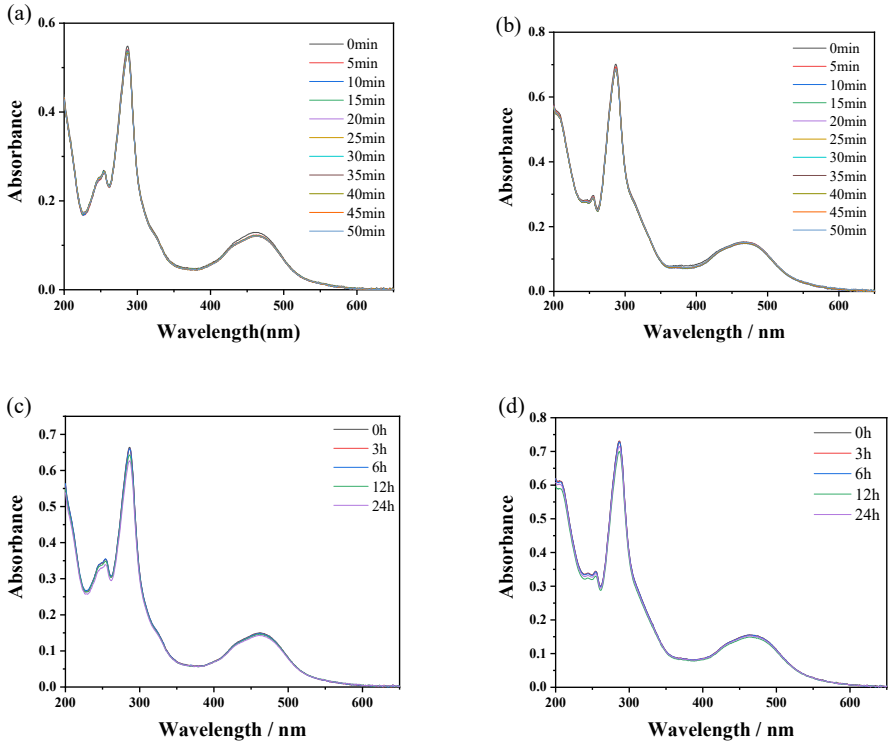

Fig. S9 (a) and (b) The photostability of **Ru-1** (10 μM) and **Ru-2** (10 μM) in aqueous solution by UV-visible absorption, respectively; (c) and (d) The stability of **Ru-1** (10 μM) and **Ru-2** (10 μM) in aqueous solution by UV-visible absorption, respectively.

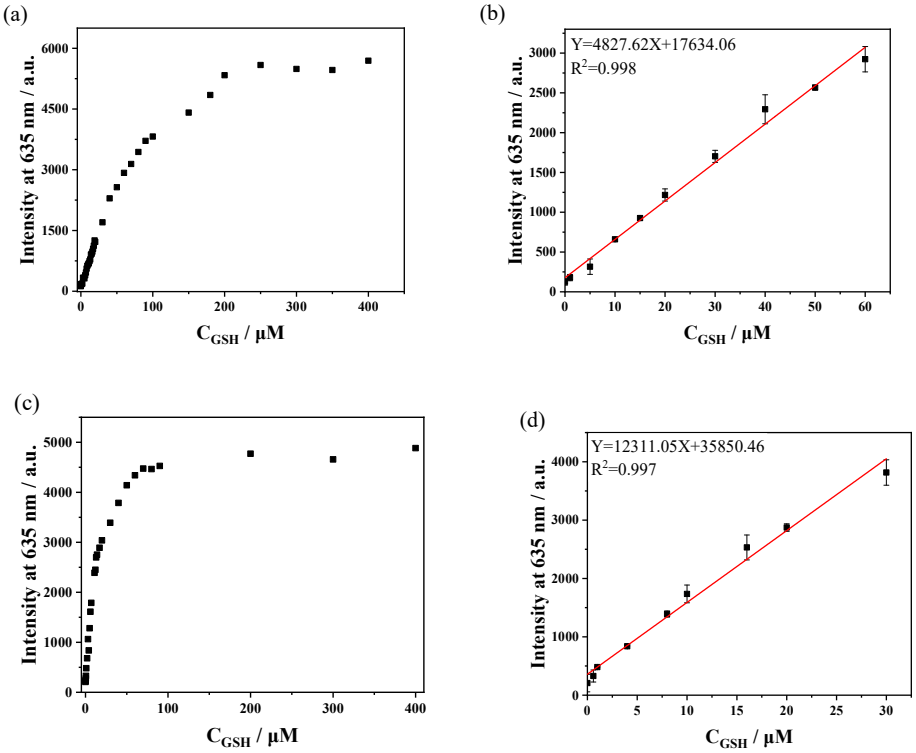

Fig. S10 (a) Variation of luminescence intensity of **Ru-1** (10 μM) and GSH (0-40 eq.). (b) Linear plot of **Ru-1** (10 μM) GSH (0-60 μM); (c) Variation of luminescence intensity of **Ru-2** (10 μM) and GSH (0-40 eq.); (d) linear plot of **Ru-2** (10 μM) and GSH (0-30 μM).

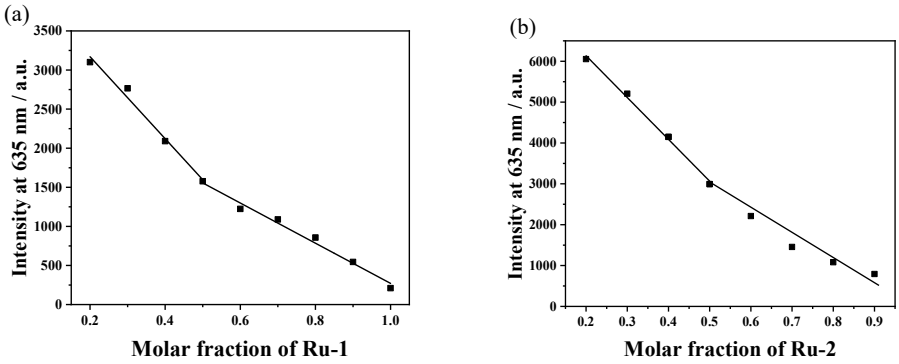

Fig. S11 (a) and (b) Luminescence plots of **Ru-1** and **Ru-2** (10 μM) in the presence of GSH at molar ratios of 1, 0.9, 0.8, 0.7, 0.6, 0.5, 0.4, 0.3 and 0.2, respectively. Phosphate buffer (10 mM, pH = 7.4), **Ru-1** (λ_{ex} = 435 nm, λ_{em} = 635 nm), **Ru-2** (λ_{ex} = 425 nm, λ_{em} = 635 nm).

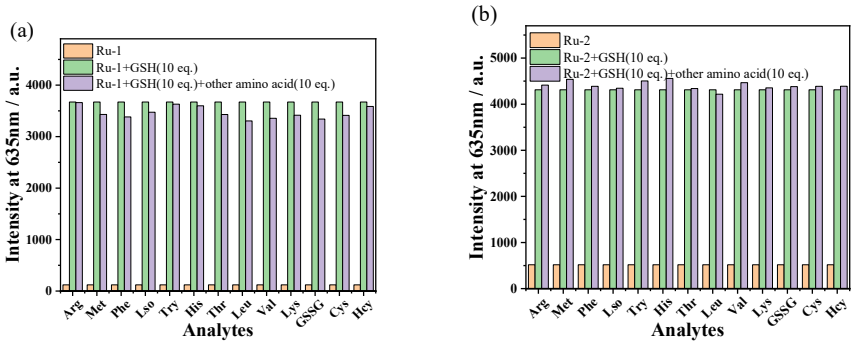

Fig. S12 (a) and (b) Luminescence plots of **Ru-1** and **Ru-2** (10 μM) against GSH (100 μM) and other amino acids (100 μM); Phosphate buffer (10 mM, pH = 7.4), **Ru-1** (λ_{ex} = 435 nm, λ_{em} = 635 nm), **Ru-2** (λ_{ex} = 425 nm, λ_{em} = 635 nm).

Mechanism

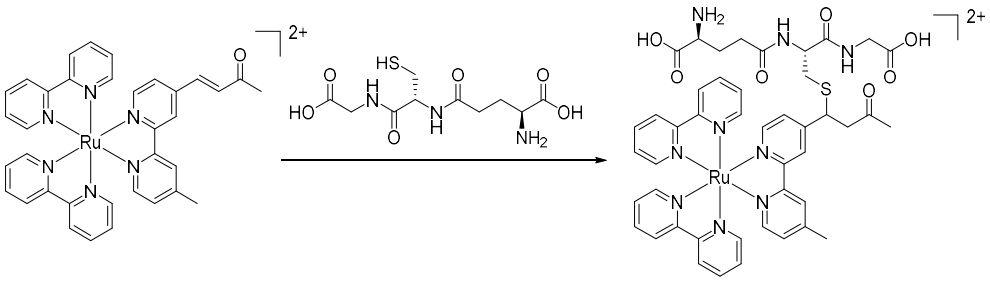

Fig. S13 Reaction of **Ru-1** with GSH in aqueous solution.

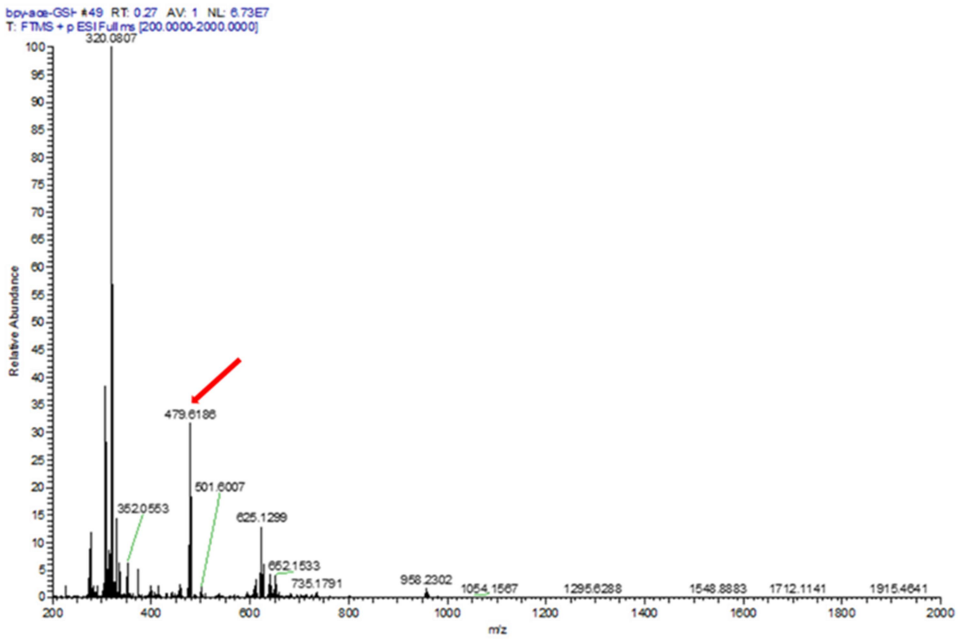

Fig. S14 ESI-MS of **Ru-1**+GSH in aqueous solution at room temperature.

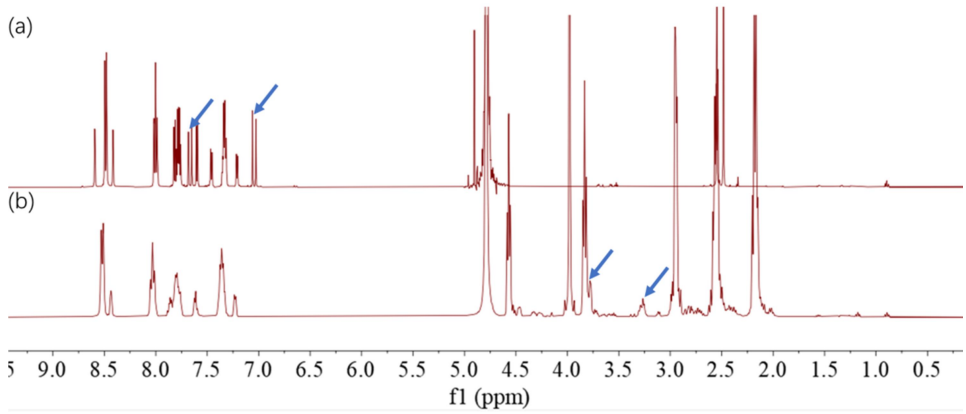

Fig. S15 ^{1}H NMR (500 MHz, D_2O-*d*) spectrum of (a) **Ru-1** and (b) **Ru-1**+GSH.

Singlet oxygen

$$\Phi_T=\Phi_{ref}\cdot S_T\cdot F_{ref}/ (S_{ref}\cdot F_t)$$

Where, the subscript T denotes the substance to be measured, and ref denotes the reference $Ru(bpy)_3^{2+}$ (Φ_{ref}= 0.56, in CH_3CN). S represents the slope of the linear fit with irradiation time as X and the change in absorbance of DPBF at 413 nm as Y.

F: Absorption correction factor; OD: Absorbance value of the co-ordinate at 450 nm.

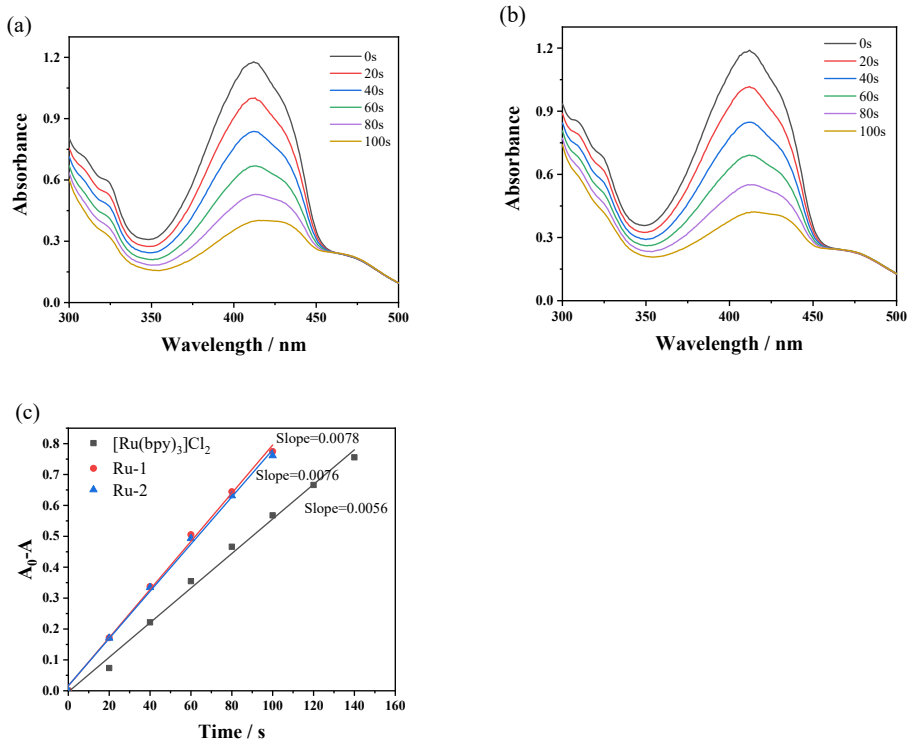

Fig. S16 (a) Absorption spectra of (a) **Ru-1** (20 μM) and (b) **Ru-2** (20 μM) with DPBF (50 μM) irradiated at 450 nm in acetonitrile solution; (c) Changes in the absorbance at 413 nm of **Ru-1**, **Ru-2** and $Ru(bpy)_3^{2+}$ with DPBF irradiated at 450 nm in acetonitrile.

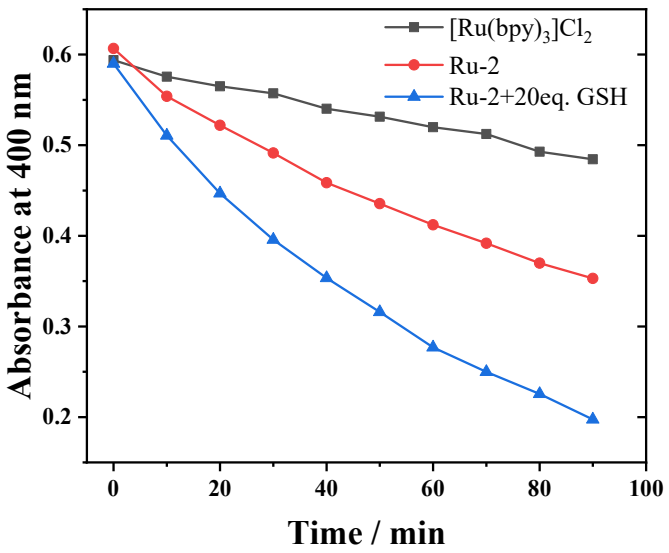

Fig. S17 Changes in the absorbance at 400 nm of $Ru(bpy)_3^{2+}$(10 μM), **Ru-2** (10 μM) and **Ru-2** (10 μM) +GSH (20eq. of complex) with ABDA (60 μM) irradiated at 450 nm in H_2O.

Table S3 IC_{50} and PI values of the complexes reported in the literature for different cell lines

Complex	Cell lines	Dark	Irradiation	PI	references
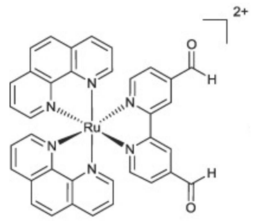	HeLa	100	81.3	1.2	2
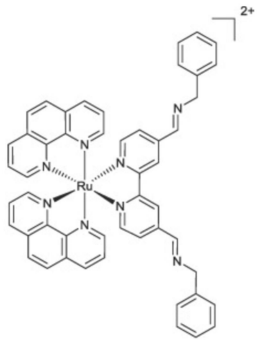	HeLa	100	18.2	5.5	2
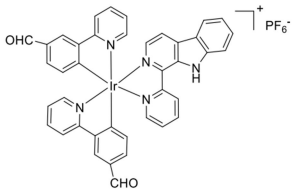	HeLa	31.3	3.8	8.24	3
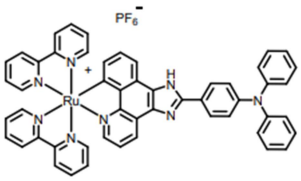	HeLa	77.48 ± 0.68	12.05± 0.33	6.4	4
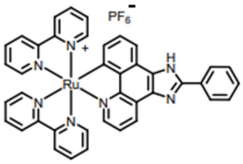	HeLa	52.1± 2.7	18.4 ± 1.1	2.8	4
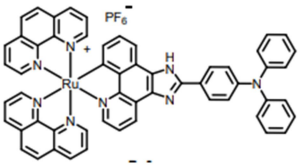	HeLa	65.3 ± 1.4	15.8 ± 1.5	4.1	4
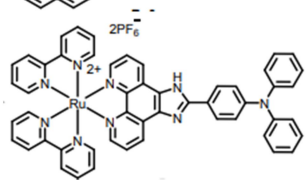	HeLa	42.2 ± 4.1	4.66± 0.40	9.1	4
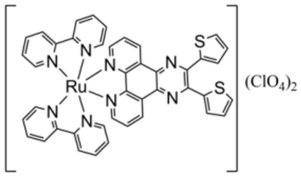	HeLa	100	21.4 ± 1.7	4.7	5

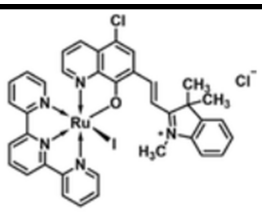	MCF-7	43 μM	3.1	13.9	6
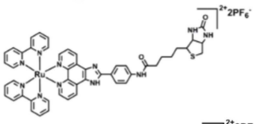	A549	＞100	1.15	87．0	7
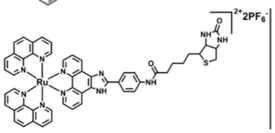	A549	＞100	0.30	333.3	7
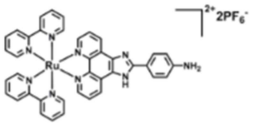	A549	＞100	82.13	1.2	7
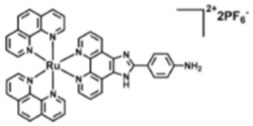	A549	＞100	71.44	1.4	7

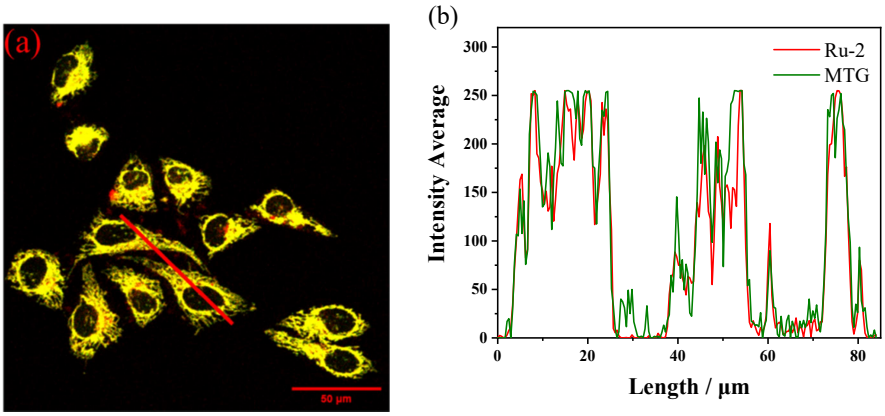

Fig. S18 (a) Merged image of co-localised fluorescence imaging of HeLa cells with Ru-2 (30 μM) and Mito-tracker Green (250 nM); (b) Intensity profiles of regions of interest (ROI) across HeLa cells.

References

1 M.-J. Li, C.-Q. Zhan, M.-J. Nie, G.-N. Chen, X. Chen, *J. Inorg. Biochem*. 2011, **105**, 420-425.

2 J. Karges, F. Heinemann, F. Maschietto, M. Patra, O. Blacque, I. Ciofini, B. Spingler, G. Gasser, *Bioorg. Med. Chem.,* 2019, **27**, 2666-2675.

3 P. Yang, S. Q. Zhang, K. Wang, H. L. Qi, Dalton Transactions 2021, **50**, 17338-17345.

4 X. Liu, G. Li, M. J. Xie, S. Guo, W. L. Zhao, F. Y. Li, S. J. Liu, Q. Zhao, *Dalton*

Trans., 2020, **49**, 11192-11200.

5 S. Q. Zhang, T. T. Meng, J. Li, F. Hong, J. Liu, Y. J. Wang, L. H. Gao, H. Zhao, K. Z. Wang, *Inorg. Chem.,* 2019, **58**, 14244-14259.

6 G. L. He, N. Xu, H. Y. Ge, Y. Lu, R. Wang, H. X. Wang, J. J. Du, J. L. Fan, W. Sun, X. J. Peng, *ACS Appl. Mater. Interfaces,* 2021, **13**, 19572-19580.

7 L. Wei, X. D. He, D. M. Zhao, M. Kandawa-Shultz, G. Q. Shao, Y. H. Wang, *Eur. J. Med. Chem.,* 2024, **264**,115985.